Effects of Size on Water Vapour Absorption and Regeneration in Lithium chloride nanocrystals

Abhinav Prakash[a], Nirmal Kumar Katiyar[b], Martha Y. Suarez-Villagran[c], John H. Miller[c], Jr., Leonardo D. Machado[d], C.S. Tiwary[e]*, Krishanu Biswas[a]*, Kamanio Chattopadhyay[f]*,*

[a]*Department of Materials Science and Engineering, Indian Institute of Technology Kanpur, Kanpur -28016, INDIA*

[b]*School of Engineering, London South Bank University, 103, Borough road, London SE10AA, United Kingdom, https://orcid.org/0000-0001-8795-7857*

[c]*Department of Physics and Texas Center for Superconductivity, University of Houston, Houston, Texas 77204-5002, United States*

[d]*Departamento de Física Teórica e Experimental, Universidade Federal do Rio Grande do Norte, Natal, Rio Grande do Norte 59072-970, BRAZIL; orcid.org/0000-0003-1221-4228; Email: leonardo@fisica.ufrn.br*

[e]*Metallurgical and Materials Engineering, Indian Institute of Technology Kharagpur, Kharagpur 721302, INDIA; orcid.org/0000-0001-9760-9768; Email: chandra.tiwary@metal.iitkgp.ac.in;*

[a]*Krishanu Biswas - Department of Materials Science and Engineering, Indian Institute of Technology Kanpur, Kanpur -28016, INDIA; kbiswas@iitk.ac.in; orcid.org/0000-0001-5382-9195.*

[f]*Department of Materials Engineering, Indian Institute of Science, Bangalore 560012, INDIA, email: kamanio@mateials.iisc.ernet.in*

Keywords: cryomilling, ionic salt, lithium chloride, mechanical milling, low temperature, regeneration, reactivation

Abstract

Ionic salts have received tremendous attention for applications such as electrolytes, solar energy, and desiccants. In particular, the high surface area of desiccant materials enhanced moisture absorption capacity, making it suitable for humidity control in various environments. However, lithium chloride (LiCl) salt properties remain largely unexplored in nanocrystalline form (at a high surface to volume ratio) due to difficulty preparing and stabilising nanoparticles, despite the high tide of expectations for energy applications. In the present investigation, for the first time, nanocrystalline LiCl was prepared by a top-down approach - successive cryomilling under an inert atmosphere. Systematic investigation shows nanocrystalline LiCl undergoes rapid dissolution in the presence of moisture. The experimental results were further corroborated with Molecular Dynamics (MD) simulations using LAMMPS. The combined use of milling at room temperature (RT) and cryomilling resulted in a crystallite size of approximately 60 nm. The nanocrystalline LiCl exhibited a water uptake capability eight times faster than that of the bulk LiCl crystal. The simulations revealed that smaller crystals are more reactive because they (i) readily deform in water and (ii) have a larger fraction of atoms with lower stability. The reasons behind the high reactivity of nanocrystalline LiCl, which has not been reported in the literature, have been discussed in detail.

1 Introduction

Lithium, the lightest alkali metal, has become a part of everyday human life in modern technological society to provide clean energy. Li and its salts are aiding in curbing the climate crisis through the use of lithium-ion batteries in current and future electric vehicles and for energy harvesting and storage [1, 2]. Such applications are aided by solid-state electrolytes[3] and molten salt synthesis of Li from low-cost LiCl[4], which is also used as a biological miticidal agent[5, 6]. Due to its unique properties, a drastic expansion of Li-ion applications is expected by 2050. The combination of Li and LiCl is unique as it exhibits various unexplained phenomena such as the dispersion of Li in LiCl producing metal fog; the solubility of Li in LiCl showing considerable variation when measured with different techniques; the thermodynamic activity of Li in the presence of LiCl being lower than unity, etc.[7]. The LiCl salt is being utilised to increase the molten salt's thermal stability for solar thermal energy storage due to its high latent heat and suitability at a high operating temperature[8]. Nanocomposites prepared for hydrogen storage include α-AlH_3/LiCl by mechanochemical synthesis[9], in which the metal hydride in nano-form stores hydrogen[10]. In addition, LiCl intercalated carbon nitride nanotubes have been prepared for lead absorption[11]. LiCl is used as a desiccant due to its super water-absorbing capability, and it is also used as an aqueous LiCl desiccant for the hybrid solar cooling system as a packed bed dehumidifier[12]. Tang *et al* [13] have reported the LiCl solution for the regeneration process and reported the increasing concentration of LiCl to decrease the regeneration rate. Similarly, the Silica-gel-LiCl composites were coated on the aluminium sheet for desiccant coated heat exchanger and found enhanced dehumidification capacity[14].

Regeneration of LiCl is possible at low temperatures (40^oC) and can be achieved using solar energy. It also supports successive cycles of absorption and regeneration[15]. These are existing applications of the lightest alkali metal. However, the nanocrystalline nature of Li/LiCl

can play a decisive role in newer applications that are yet to mature. Renewable energy companies and research groups have been experimenting with these for the past few years and have accelerated the development of new applications and technologies. For many years, solar energy has been used to power cooling devices to combat the summer heat and has a high potential for small-scale energy production. For example, an absorption machine like a heat pump powered by solar energy generates lower temperatures. which is costly and has lower efficiency. The LiCl absorbs moisture and suffers losses during continuous usage in the reactor. It is well known that the reactivity of the ionic crystal, such as KCl, can be increased by introducing defects that enhance the absorption of water, and at the same time, react with water faster due to its small size[16, 17].

None of the previous investigations has explored nanoparticles of LiCl and their behaviour due to challenges in preparation. In addition, the hygroscopic nature makes processing complex and costly. Therefore, we used cryomilling cum room temperature ball milling to prepare LiCl nanoparticles. The nanoparticle sizes and morphologies versus milling time were investigated, with an evaluation of variations in absorption/regeneration capability as a function of particle size. Finally, we performed molecular dynamics simulations to assess the high reactivity of nanocrystalline LiCl with water.

2 Experimental section

Materials and method

The pure lithium chloride anhydrous (99%) ionic salt with a -20 mesh size from Alfa Aesar® is used for milling. Mechanical milling was carried out in two steps. The sample was initially milled at low temperature in a specially designed vibratory cryomill (below 123 K[18-22]) using a ball to powder weight ratio (BPR) of 100:1. The coolant liquid nitrogen (LN_2) was introduced in the surrounding of the milling jar, such that milling materials and coolant never get mixed and milling powder remains dry. The samples were collected at different time

intervals (1-6 hours) to probe crystallite size reduction. The 6-hour milled sample was further mechanically milled at room temperature using a P7 mill (Planetary Micro Mill, Pulverisette, Fritsch, Germany) at an rpm of 400 and keeping the ball to powder weight ratio at 50:1. In addition, sufficient precautions were taken to avoid contact with moisture and/or impurities. Since Lithium chloride is highly deliquescent, the samples were stored in a high vacuum desiccator to minimise moisture.

Characterisations

After milling, the particle size was determined using a Transmission Electron Microscope (TEM; Technai F30) operated at 300 kV. The images were recorded rapidly to avoid radiation damage from the electron beam. The morphology of LiCl crystals was evaluated using scanning electron microscopy (FEI SERION, Field emission), and extra precautions were taken to avoid environmental exposure to the samples. The rate of moisture uptake and loss of moisture by different crystals size of LiCl was estimated using Thermogravimetry analysis (TGA). Initially, the experiment was performed at 30^{o}C, and later it was heated up to 100^{o}C, and the moisture loss was recorded. The fractional increase in the mass of LiCl per unit surface area was plotted against time to quantify the changes in absorption properties of LiCl with particle size. Similarly, the effect of moisture absorption on the morphology and the behaviour of the surface with different particle sizes was investigated through optical images taken at intervals of 1 second using (*NIKON Z50*). The imaging was carried out from the beginning to capture the early-stage changes in the morphology.

Simulations

Molecular Dynamics (MD) simulations were carried out to gain atomistic insight into how size affects the interaction between water and LiCl nanocrystals. The calculations were performed using the CHARMM[23] force field within the LAMMPS[24] software. In addition, the TIP3P

model[25] was used to simulate the water. Two types of simulations were executed using distinct methodologies.

In the first type, the dissolution of LiCl crystals in water was simulated with a 20.4 Å x 20.4 Å x 20.4 Å non-periodic crystal (total surface area: 2500 $Å^2$). Then we surrounded LiCl with 28121 water molecules (see Figure 4(a)) and added periodic boundary conditions to the LiCl+ water system. We used a crystal periodic in two directions (Lx = Ly = 55.6 Å) and non-periodic in the third (Lz = 20.2 Å) to simulate a large crystal. Then we surrounded one of the crystal faces with 27801 water molecules and added a Lennard-Jones wall to confine the water in the z-direction. The total length of the water column for this instance was 305 Å, and the water-crystal contact area was 3090 $Å^2$. Furthermore, the two rows of LiCl atoms farther from the water were kept frozen.

Part of this structure is displayed in Figure 4(b) (only a small fraction of all water molecules is shown). Note that we designed the structures with similar surface areas, as dissolution rates should depend on the surface area. We used a time step of 1 femtosecond to evolve this system in time. All simulated systems were equilibrated in the NPT ensemble for 100000 steps using P = 1 atm and T = 300 K. Then, the thermostat and barostat were turned off, and the system was evolved for 10000000 steps in the NVE ensemble.

The energy required to remove atoms from certain positions in a LiCl crystal was calculated in the second type. As in previous simulations, a crystal size of 20.4 Å x 20.4 Å x 20.4 Å was used. Before starting the calculations, we added periodic boundary conditions to the solid, minimised its energy using the conjugate gradient method for 5000 steps, and equilibrated the system in the NPT ensemble for 100000 steps. The conditions P = 1 atm and T = 300 K were used. Then six atoms (3 Li and 3 Cl) were selected and removed from the crystal in a direction perpendicular to it (see Figure 5(a-b). The considered atoms were in different positions of the

cubic crystal: (i) in the face, (ii) in the edge, (iii) in the vertex. In the results, zero energy corresponds to a configuration where the removed ion is far from the crystal (50 Å).

3 Results and Discussion

The successive cryomilling and room temperature (RT) milling resulted in LiCl nanoparticles. These nanoparticles are endowed with exceptional absorption and regeneration ability compared to their bulk counterpart. The experimental scheme is shown in Figure 1(a). The successive milling of alkali salt at cryogenic temperature followed by room temperature significantly reduces particle size compared to either only cryomilling or room-temperature milling[16, 17, 26-28]. The cryomilling suppresses the recovery, and brittle fracture dominates due to a lack of defect generation at lower temperatures[21]. On the contrary, room temperature milling enhances defect generation and annihilation, leading to extensive size reduction of Lithium chloride salts [16, 26]. The morphology of as received Lithium chloride has shown in Figure 1(b); after cryomilling (6 hr), the crystallites get reduced to below ~100 nm, as shown in Figure 1(c). The mode of the particle size distribution is 60nm with a wide distribution, as shown in Figure 1(f). Room temperature milling for 50 hr further reduced the crystallite size to approximately ~50 nm, with particles achieving an octahedral shape, as shown in Figure 2(g).

Absorption/regeneration

The hygroscopic materials actively absorb moisture from their surroundings and enhance their weight (mass gain). The water molecules/moisture uptake or absorption depends on the affinity of salt molecules to the water molecules. Thus, the alkali salts (LiCl, NaCl, KCl, etc.) undergo a chemical change by absorbing water. It holds the water and turns from a solid to an aqueous desiccant solution (LiCl)[29]. The LiCl absorbing water is an exothermic reaction and readily dissociates into its ionic form[30]. Although the nanoparticles have unique properties

compared to their bulk counterparts due to the high surface area to volume ratio[31], the behaviour of nanocrystalline LiCl is largely unknown.

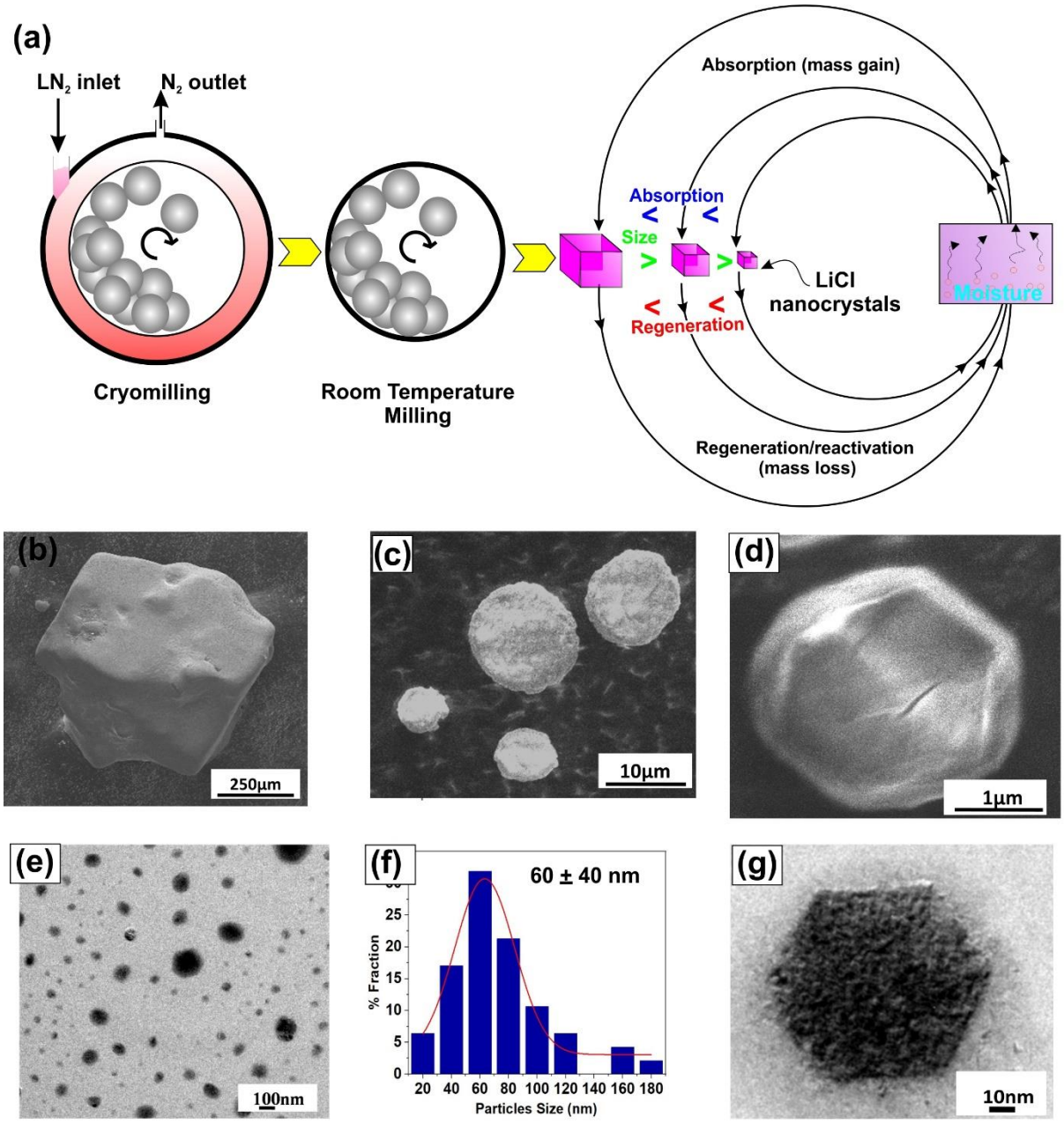

Figure 1: **(a)** Schematic of the experimental scheme (successive cryo-RT milling and LiCl absorption-regeneration); **(b)** SEM micrograph LiCl as received crystal; **(c)** SEM micrograph of 6 hours cryomilled LiCl; **(d)** SEM image of a particle subjected to combined milling (6 hours cryo + 50 hour RT milling); **(e)** TEM bright-field image of distribution of particles cryomilled for 6 hours, **(f)** the particles size distribution of image e **(g)** TEM bright-field image of a particle subjected to combined milling (6 hours cryo + 50 hour RT milling).

Therefore, the effect of particle size on the hygroscopic nature of LiCl is expected. Hence, a quantitative relationship between the fractional increase in mass per unit surface area (Δm/A) and time (t) can be established as under:

$$\log\left(\frac{\Delta m}{A}\right) = n\log t + \log k \qquad (1)$$

simplifying

i.e. $$\frac{\Delta m}{A} = kt^n \qquad (2)$$

We denote *n* as the time exponent and *k* as the time coefficient.

The mass gain/loss per unit surface was recorded for different particles size of LiCl with time using thermogravimetry, as shown in Figure 2. The nanocrystalline LiCl has more linear water absorption behaviour with time, while the bulk crystal exhibits a parabolic behaviour absorption reducing with more extended time. In the case of regeneration, the nanocrystalline material follows a smooth decreasing trend of the mass fraction with time. However, the mass gain is higher, and mass loss is lower in nanocrystalline LiCl than in bulk, as shown in Figure 2(e). To obtain more precise information, linear fittings were performed using equation 2 to extract the values of *n* and log *k*, which were subsequently plotted against the measured particle sizes. The variation in their values is shown in Figure 3(a). As the figure shows, the values of time exponent (n) and time coefficient (k) depend greatly on particle sizes.

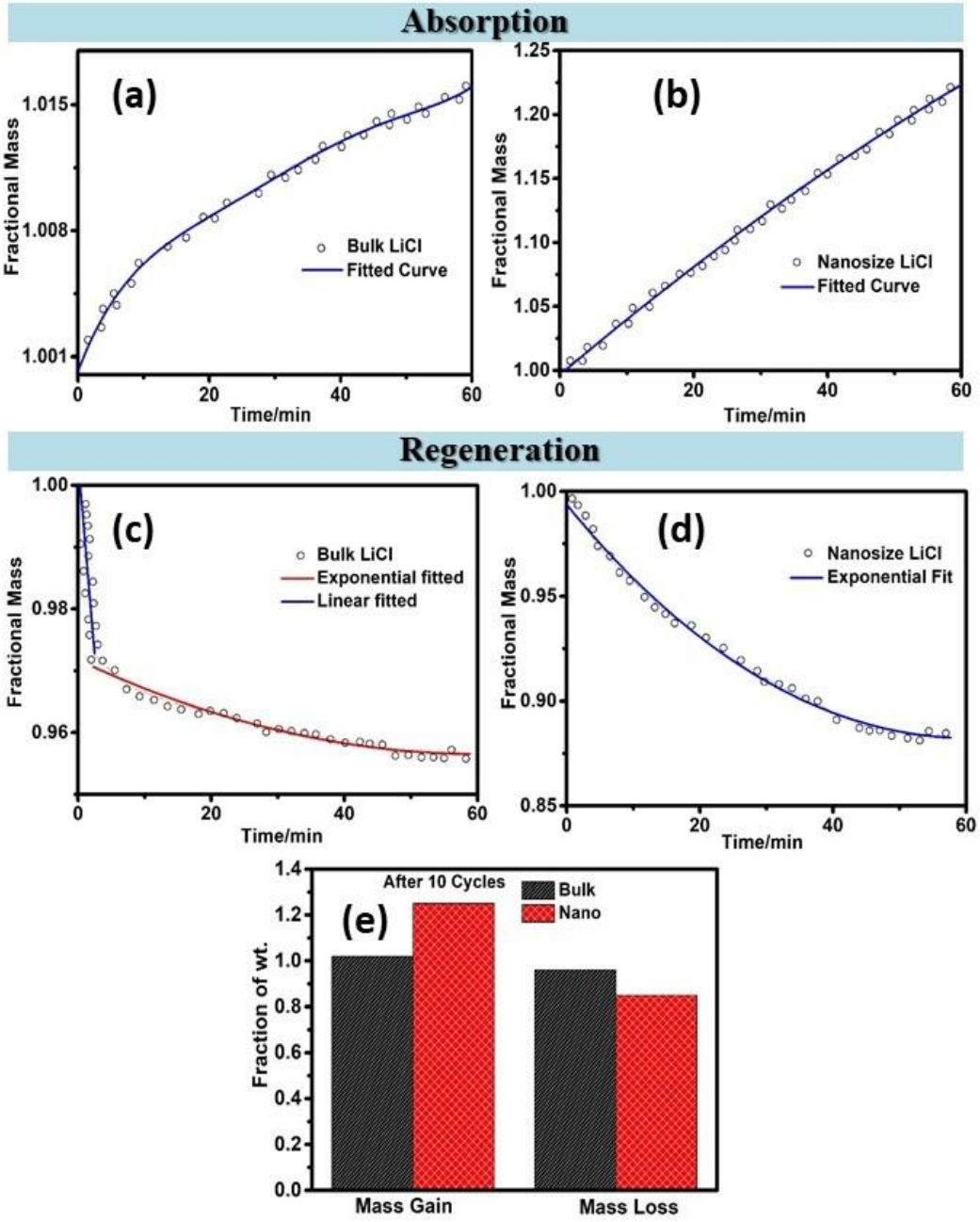

Figure 2: Absorption (gain of fractional mass ($\Delta m/A$)), and regeneration (loss of fractional mass ($\Delta m/A$)) of LiCl with respect to time; **(a)** absorption in LiCl bulk crystal; **(b)** absorption in LiCl nanocrystals; **(c)** regeneration of LiCl bulk crystal; **(d)** regeneration of LiCl nanocrystals; **(e)** comparison of absorption (mass gain), regeneration (mass loss) of bulk and nanocrystal respectively.

Since the surface area term has already been incorporated in ($\Delta m/A$), particle activity probably also contributes to lithium chloride's overall reactivity/absorption capacity. The plot shows that n varies approximately between 0.5 and 1.5 for different particle sizes. The experimental results

for our samples indicate that $n \approx 0.6$ for the bulk LiCl crystals, whereas for the nanosized ionic crystal, its value remains close to 1.

Differentiating the above equation, Eq. 2, we get:

$$\frac{d(\frac{\Delta m}{A})}{dt} = knt^{(n-1)}$$

Therefore, for $n \approx 1$, which is the case for nanosized ionic crystals, the absorption rate is independent of time, *i.e.*, a nanoparticle can continue absorbing moisture at the same rate as it was initially until it becomes fully saturated. On the other hand, for bulk particles, the rate decreases continuously with time as $n < 1$. It is illustrated in the linear and parabolic nature of the plots in Figure 2(a-d).

For regeneration, the specimens were heated up to 100°C and kept at this temperature for the particles to lose their water content. Due to their increased surface area, the nanosized ionic crystals get rid of their moisture faster than the bulk ionic crystals of LiCl. Thus, the smaller particles can be recycled much more efficiently than larger ones, increasing the reproducibility of the reactant. To determine the role of activity in LiCl absorption/regeneration enhancement at nanoscale particle size, we consider the following.

Let consider,

$$LiCl\ (s) \quad \rightarrow \quad LiCl(s) \qquad \ldots(3)$$

For solid specimens (eq. 3), activity is defined as follows[32]:

$$a_{LiCl} = f_{LiCl} x_{LiCl} \qquad \ldots(4)$$

f_{LiCl} is an activity coefficient; x_{LiCl} is a mole fraction. For pure LiCl (without any water content), f_{LiCl} and x_{LiCl} both equal to 1, *i.e.*, the activity is unity. For simplicity, we will assume the following:

1. The activity coefficient f_{LiCl} remains unchanged with moisture absorption (which is not valid, but for our calculations, this will suffice).
2. The above equation (4) holds for LiCl even after moisture absorption.

When there is a change in mass (Δm) due to water, we can write the mole fraction as follows:

$$x_{LiCl} = \frac{m_{LiCl}/M_{LiCl}}{m_{LiCl}/M_{LiCl} + m_{H_2O}/M_{H_2O}} \quad \ldots (5)$$

where, m_{H_2O} = Δm = Akt^n. Our measurements show that even though Δm/A is orders of magnitude smaller for nanosized ionic crystals, the fractional change in mass of LiCl, Δm is about ten times larger than bulk ionic crystals after 1 hour of absorption time due to an enormous increase in surface area, A in the nanoscale (Figure 3(b)). The activity being directly proportional to mole fraction, which in turn is inversely proportional to Δm, we conclude that LiCl activity decreases to a lower value for nanosized ionic crystals than for the bulk.

On absorbing moisture, Lithium chloride undergoes the following chemical reaction:

$$LiCl\ (s) + H_2O\ (l) \rightarrow LiOH\ (s) + HCl\ (l) \quad \ldots(6)$$

The equilibrium constant and the standard Gibbs energy (ΔG^o) change for this reaction can thus be written as

$$k = \frac{a_{LiOH} a_{HCl}}{a_{LiCl} a_{H_2O}}$$

$$\Delta G^o = -RT \ln k = -RT \ln \frac{a_{LiOH} a_{HCl}}{a_{LiCl} a_{H_2O}}$$

Consequently, a decrease in the value of a_{LiCl} will make the free energy change even more negative, leading to a more favourable reaction in the case of nanosized ionic crystals. It explains why the rate of absorption is greater for nanoparticles. Further, a visual experiment was performed to probe the effect of moisture absorption on nanocrystalline LiCl and bulk LiCl. Figure 3(c) shows how the crystals of lithium chloride change their morphology with time for two different particle sizes of LiCl. The first sequence of images (bulk LiCl) represents the as received LiCl crystals. In contrast, the second sequence (Nanocrystalline LiCl) is that of LiCl cryomilled for 6 hours, followed by room temperature milling for 50 hours. As is evident from these images, the total time required for the complete disappearance of the particles (melting by absorbing moisture from the atmosphere due to the deliquescent nature of LiCl) is much smaller (approximately an order less) for nanosized ionic crystals in comparison to that for bulk crystals.

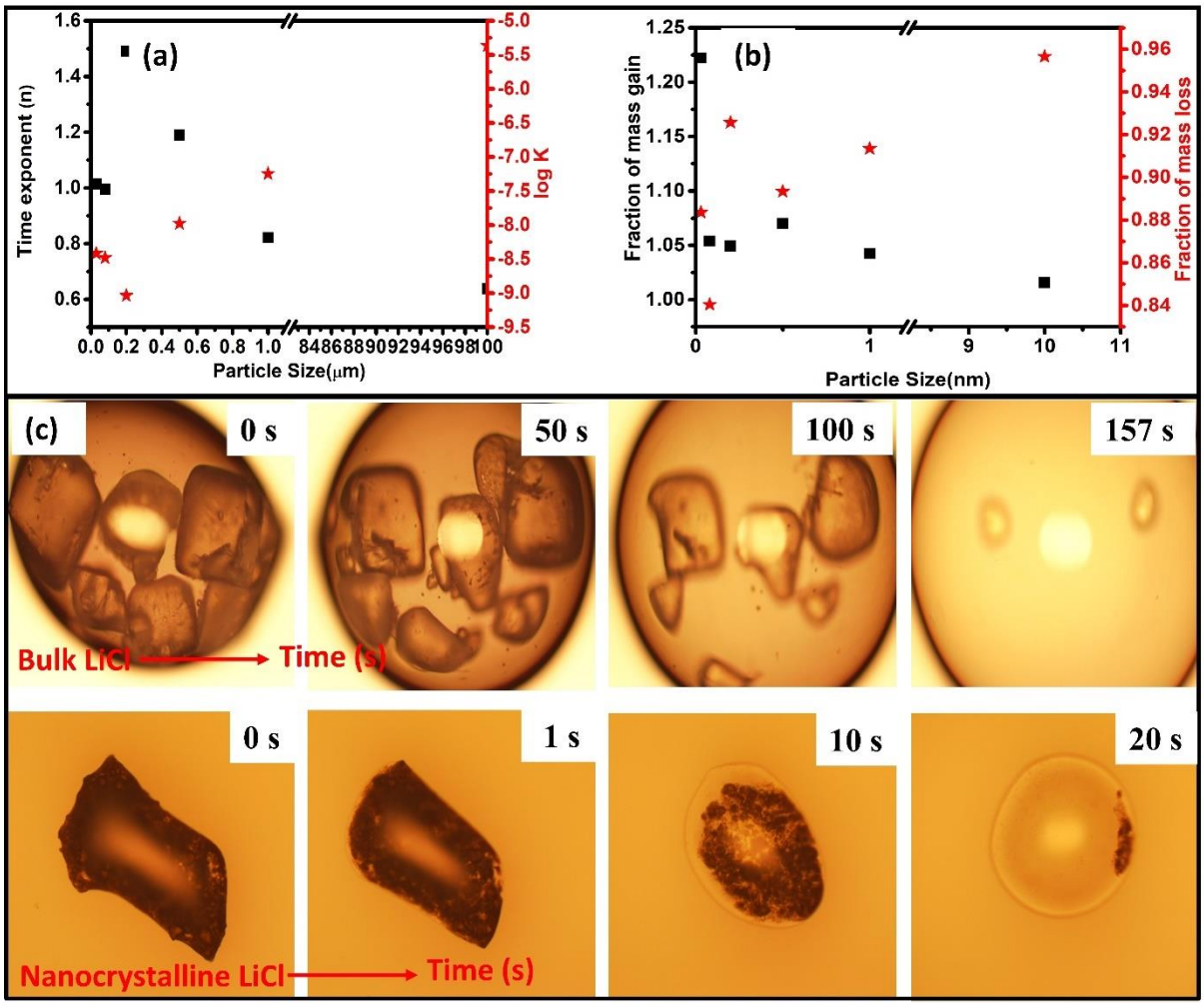

Figure 3: (a) Time exponent and log k with respect to particle size; **(b)** Fraction of mass gain and mass loss with respect to particle size, **(c)** Optical image of bulk and nanocrystalline LiCl absorption of water with respect to time (time mentioned over each image right upper corner) until complete dissolution.

LiCl dissolution simulations

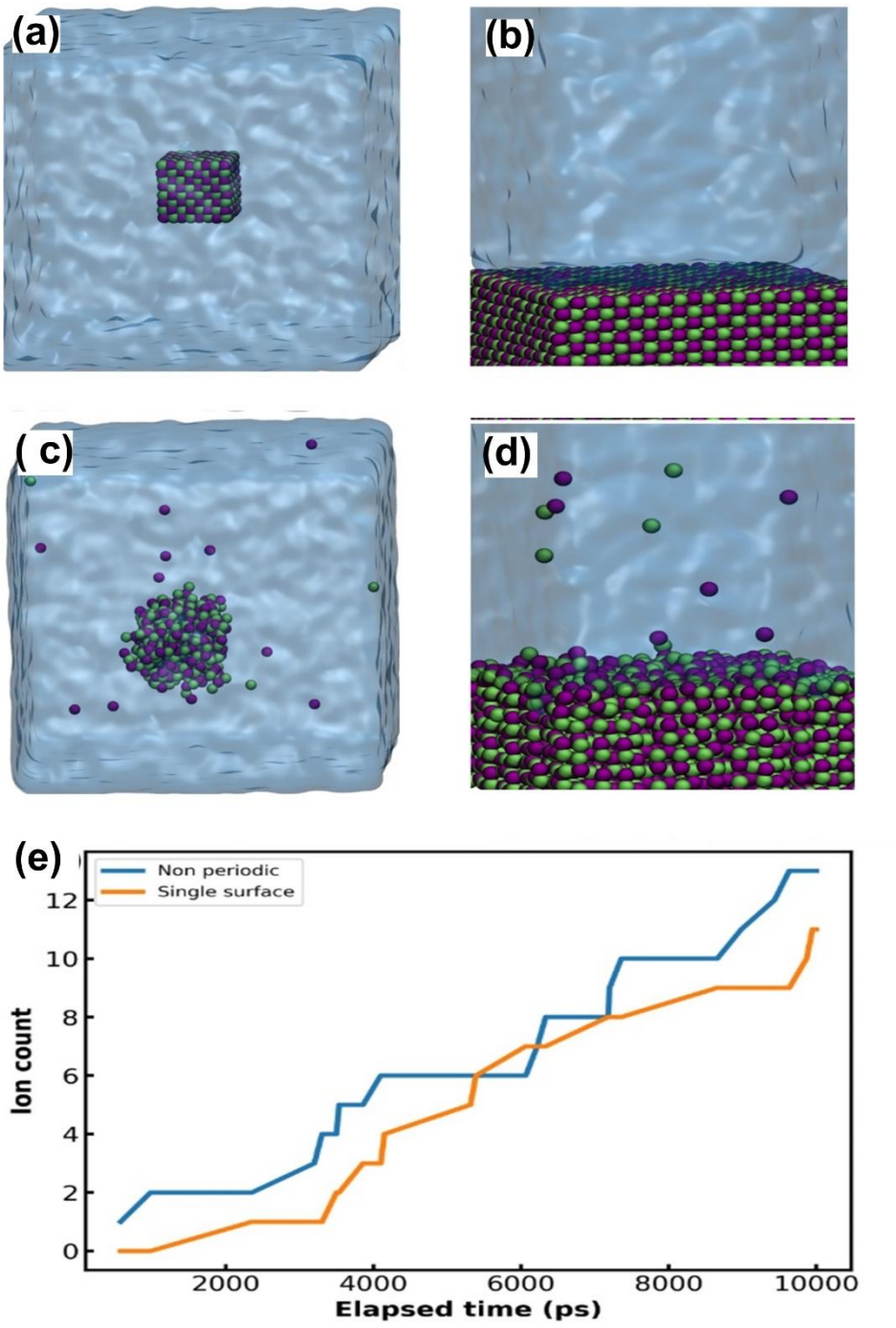

Figure 4: (a-b) present the initial configuration for the non-periodic and the single surface crystal, **(c-d)** display the same structures after the completion of the MD simulations, **(e)** shows the number of ions dissolved in water over time (In this graph, we only counted ions that remained diffused in water until the end of the simulation).

Figure 4 shows the results of the simulations of LiCl dissolution in water. Figure 4(a) and (b) display the initial configuration for the non-periodic crystal and the single surface crystal. In contrast, Figure 4(c) and (d) present the final arrangements after ten nanoseconds of MD simulation. Note that the non-periodic crystal is distorted at the simulation end, while the single surface crystal partially retains its original shape. To examine the dissolution rate, we counted the number of ions dissolved in the water over time. We present the results in Figure 4(e). One important note is that some ions, dissolved in the water, eventually diffuse back to the crystal. In Figure 4(e), we did not count those ions and considered only those remaining dissolved until the simulation ended. This process occurred more frequently for the non-periodic crystal, possibly because the water column length is relatively small in all directions. The behaviour can be observed in detail with Supplementary Movies S1 and S2, displaying ten nanoseconds long atomic trajectories. It is to be noted that the non-periodic crystal dissolved faster than the single surface crystal, even though its contact area with the water was smaller, as displayed in Figure 4(e). We note that the non-periodic structure mimics a small LiCl crystal, while the structure with a single surface mimics a large crystal. In that case, we conclude that the simulation and experimental results agree. Recall that while we expect an increased mass loss for smaller LiCl crystals in water, the experiments found that the increased surface area could not entirely account for the measured increase in mass loss. To understand this effect, we determined the energy required to remove an atom from different positions in the LiCl crystal.

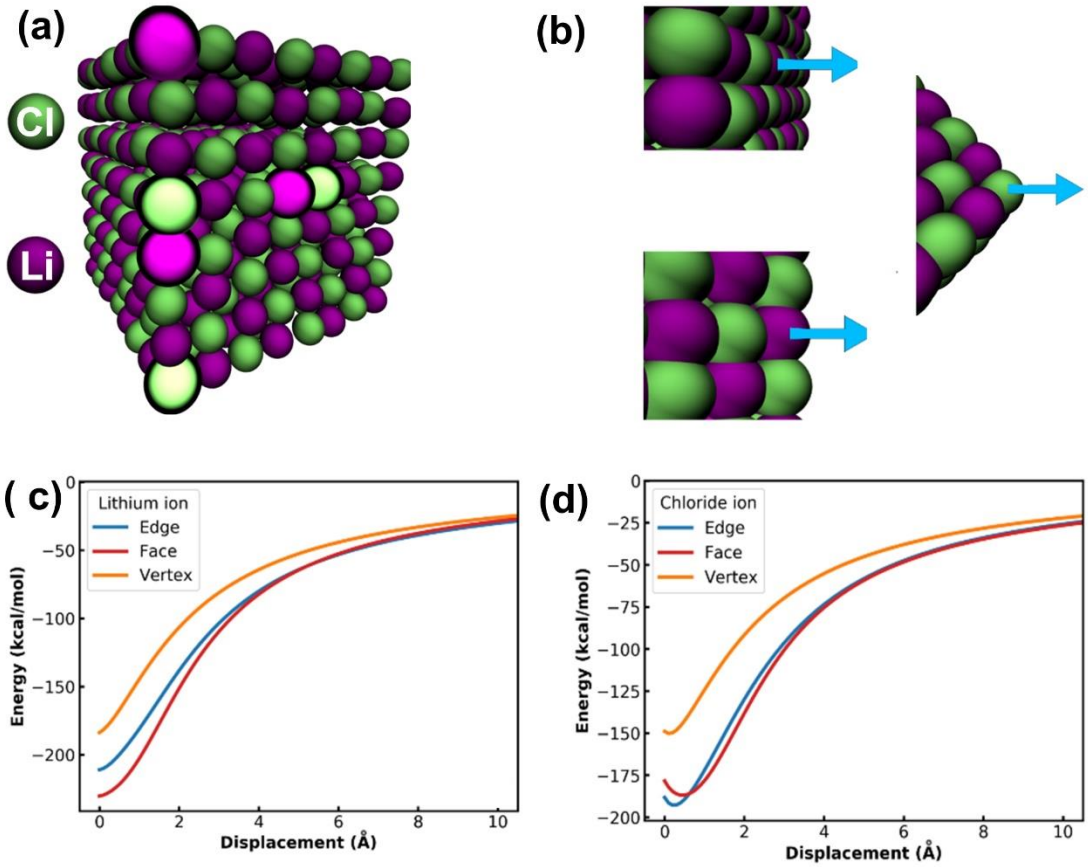

Figure 5: (a) LiCl crystal after optimisation and equilibration at 300 K. The six highlighted atoms correspond to those removed from the structure to obtain the energy curves presented in **(c)** and **(d)**. We displaced each atom in a direction perpendicular to the crystal, as illustrated in **(b)**.

The Li and Cl atoms were removed from three different positions: (i) face, (ii) edge, (iii) vertex (see Figure 5(a)). To remove these atoms, we displaced them perpendicular to the crystal, see Figure 5(b). The results for Lithium and Chloride ions are presented in Figure 5(c) and (d), respectively. In both cases, notice that ions in the vertex position are bound more weakly to the crystal (the energy is less negative). For Lithium, edge ions' binding energy is smaller than face ions. In contrast, for Chloride, the binding energy for face and edge ions is approximately the same. Although these energy calculations are simplified (water molecules were not included), their results correlate well with the MD simulations for the non-periodic crystal, where atoms in the vertex position were the first to dissolve in water. Notice that atoms in the vertices and

edges correspond to a larger fraction of the total for smaller crystals. Hence, in the picture suggested by the calculations, dissolution starts in the vertices and edges of the crystal, where the binding energy is lower. Then, the ensuing defects likely decrease the stability of adjacent atoms. Finally, smaller crystals deform readily inside the water, and the reduced order further facilitates the diffusion of ions into the liquid. The described effects add up, increasing the dissolution rate of smaller crystals.

4 Conclusion

In conclusion, this study presents a cost-effective and straightforward method for preparing lithium chloride (LiCl) salt nanoparticles by employing cryomilling and room temperature milling techniques. The successive application of these milling approaches has reduced the average particle size of LiCl to ~60 nm. Notably, the reactivity of LiCl with water was eight times increased compared to bulk LiCl crystals, attributed to alterations in LiCl activity that facilitated a more efficient water absorption reaction in LiCl nanoparticles.

Molecular dynamics simulations provided further evidence, demonstrating that smaller LiCl crystals exhibited accelerated dissolution rates in water compared to equivalent portions of larger crystals with similar surface areas. This enhanced reactivity can be attributed to the smaller crystals' greater deformability in water and a higher fraction of atoms occupying less stable vertex and edge positions.

The synthesised LiCl nanoparticles hold great potential for various nanocomposite applications in hydrogen storage, including metal hydride synthesis, solid electrolytes, solid desiccants, and more. The combination of cryomilling and conventional ball milling techniques showcased their effectiveness in the nanoparticle preparation of hygroscopic ionic solids.

The cryomilling in a dry environment of hygroscopic materials paved the way for the development of advanced nanocomposites in the field of hydrogen storage and related areas.

Future studies may focus on optimising the synthesis techniques and exploring the incorporation of LiCl nanoparticles into specific applications. By further investigating LiCl nanoparticles' unique

properties and applications, it will be possible to unlock their full potential and advance the development of innovative materials for various energy-related fields.

ASSOCIATED CONTENT

Supporting Information

Simulation movie S1 and S2

Acknowledgement:

KB would like to thank various funding agencies, the Science and Engineering Research Board under the aegis of the Department of Science and Technology (DST) India, Indian Space Research Organization (ISRO) India and IIT Kanpur for experimental facilities. CST would like to thank Science and Engineering Research Board (SERB) Ramanujan Fellowship. KC will like to thank SERB for its distinguished fellowship and National Science Chair. NKK would like to acknowledge the Newton Fellowship award from the Royal Society (Grant No.NIF\R1\191571)

References

[1] A. Manthiram, A reflection on lithium-ion battery cathode chemistry, Nat. Commun. 11(1) (2020) 1550.

[2] C. Xu, Q. Dai, L. Gaines, M. Hu, A. Tukker, B. Steubing, Future material demand for automotive lithium-based batteries, Commun. Mater. 1(1) (2020) 99.

[3] H. Ogawa, H. Mori, Lithium salt/amide-based deep eutectic electrolytes for lithium-ion batteries: electrochemical, thermal and computational study, Phys. Chem. Chem. Phys. 22(16) (2020) 8853-8863.

[4] J. Lang, Y. Jin, K. Liu, Y. Long, H. Zhang, L. Qi, H. Wu, Y. Cui, High-purity electrolytic lithium obtained from low-purity sources using solid electrolyte, Nat. Sustain. 3(5) (2020) 386-390.

[5] B. Ziegelmann, E. Abele, S. Hannus, M. Beitzinger, S. Berg, P. Rosenkranz, Lithium chloride effectively kills the honey bee parasite Varroa destructor by a systemic mode of action, Sci. Rep. 8(1) (2018) 683.

[6] J.W. Choi, D. Aurbach, Promise and reality of post-lithium-ion batteries with high energy densities, Nat. Rev. Mater. 1(4) (2016) 16013.

[7] A. Merwin, W.C. Phillips, M.A. Williamson, J.L. Willit, P.N. Motsegood, D. Chidambaram, Presence of Li Clusters in Molten LiCl-Li, Sci. Rep. 6(1) (2016) 25435.

[8] T.O. Dunlop, D.J. Jarvis, W.E. Voice, J.H. Sullivan, Stabilization of molten salt materials using metal chlorides for solar thermal storage, Sci. Rep. 8(1) (2018) 8190.

[9] D. Congwen, C. Yizheng, H. Lianxi, Z. Yuling, F. Dong, M. Jinlong, Z. Jinghong, Mechanochemical synthesis of the α-AlH3/LiCl nano-composites by reaction of LiH and AlCl3: Kinetics modeling and reaction mechanism, Int. J. Hydrog. Energy 44(42) (2019) 23716-23725.

[10] C.W. Duan, L.X. Hu, J.L. Ma, Ionic liquids as an efficient medium for the mechanochemical synthesis of α-AlH3 nano-composites, J. Mater. Chem. A 6(15) (2018) 6309-6318.

[11] Y. Zhou, C. Liao, Y. Fan, S. Ma, M. Su, Z. Zhou, T.-S. Chan, Y.-R. Lu, K. Shih, Highly crystalline lithium chloride-intercalated graphitic carbon nitride hollow nanotubes for effective lead removal, Environ. Sci. Nano 6(11) (2019) 3324-3335.

[12] N. Fumo, D.Y. Goswami, Study of an aqueous lithium chloride desiccant system: air dehumidification and desiccant regeneration, Solar Energy 72(4) (2002) 351-361.

[13] C. Tang, X. Qian, B. Tan, Z. Yuan, Y. Huang, A novel analysis of LiCl solution regeneration experiments, Case Stud. Therm. Eng. 39 (2022) 102397.

[14] X. Zheng, T.S. Ge, Y. Jiang, R.Z. Wang, Experimental study on silica gel-LiCl composite desiccants for desiccant coated heat exchanger, Int. J. Refrig. 51 (2015) 24-32.

[15] K.S. Rambhad, P.V. Walke, D.J. Tidke, Solid desiccant dehumidification and regeneration methods—A review, Renew. Sustain. Energy Rev. 59 (2016) 73-83.

[16] C.S. Tiwary, A. Verma, K. Biswas, A.K. Mondal, K. Chattopadhyay, Preparation of ultrafine CsCl crystallites by combined cryogenic and room temperature ball milling, Ceram. Int. 37(8) (2011) 3677-3686.

[17] P. Sharma, K. Biswas, A.K. Mondal, K. Chattopadhyay, Size effect on the lattice parameter of KCl during mechanical milling, Scripta Materialia 61(6) (2009) 600-603.

[18] N. Kumar, K. Biswas, Fabrication of novel cryomill for synthesis of high purity metallic nanoparticles, Rev. Sci. Instrum. 86(8) (2015) 083903-8.

[19] K. Barai, C.S. Tiwary, P.P. Chattopadhyay, K. Chattopadhyay, Synthesis of free standing nanocrystalline Cu by ball milling at cryogenic temperature, Mater. Sci. Eng. A 558(0) (2012) 52-58.

[20] N. Kumar, K. Biswas, R.K. Gupta, Green synthesis of Ag nanoparticles in large quantity by cryomilling, RSC Advances 6(112) (2016) 111380-111388.

[21] N.K. Katiyar, K. Biswas, C.S. Tiwary, Cryomilling as environmentally friendly synthesis route to prepare nanomaterials, Int. Mater. Rev. 66(7) (2020) 493-532.

[22] N.K. Katiyar, K. Biswas, C.S. Tiwary, L.D. Machado, R.K. Gupta, Stabilization of a Highly Concentrated Colloidal Suspension of Pristine Metallic Nanoparticles, Langmuir 35(7) (2019) 2668-2673.

[23] A.D. MacKerell, D. Bashford, M. Bellott, R.L. Dunbrack, J.D. Evanseck, M.J. Field, S. Fischer, J. Gao, H. Guo, S. Ha, D. Joseph-McCarthy, L. Kuchnir, K. Kuczera, F.T.K. Lau, C. Mattos, S. Michnick, T. Ngo, D.T. Nguyen, B. Prodhom, W.E. Reiher, B. Roux, M. Schlenkrich, J.C. Smith, R. Stote, J. Straub, M. Watanabe, J. Wiórkiewicz-Kuczera, D. Yin, M. Karplus, All-Atom Empirical Potential for Molecular Modeling and Dynamics Studies of Proteins, J. Phys. Chem. B 102(18) (1998) 3586-3616.

[24] S. Plimpton, Fast Parallel Algorithms for Short-Range Molecular Dynamics, J. Comput. Phys. 117(1) (1995) 1-19.

[25] D.J. Price, C.L. Brooks, A modified TIP3P water potential for simulation with Ewald summation, J. Chem. Phys. 121(20) (2004) 10096-10103.

[26] A. Verma, K. Biswas, C. Tiwary, A. Mondal, K. Chattopadhyay, Combined Cryo and Room-Temperature Ball Milling to Produce Ultrafine Halide Crystallites, Metall. Mater. Trans. A 42(4) (2011) 1127-1137.

[27] C. Tiwary, A. Verma, S. Kashyp, K. Biswas, K. Chattopadhyay, Preparation of Freestanding Zn Nanocrystallites by Combined Milling at Cryogenic and Room Temperatures, Metall. Mater. Trans. A 44(4) (2013) 1917-1924.

[28] C.S. Tiwary, S. Kishore, R. Vasireddi, D.R. Mahapatra, P.M. Ajayan, K. Chattopadhyay, Electronic waste recycling via cryo-milling and nanoparticle beneficiation, Materials Today 20(2) (2017) 67-73.

[29] A. ASHRAE, Handbook of fundamentals, American Society of Heating Refrigerating and Air Conditioning Engineers, Atlanta, GA (2005).

[30] C. Monnin, M. Dubois, N. Papaiconomou, J.-P. Simonin, Thermodynamics of the LiCl + H2O System, J. Chem. Eng. Data 47(6) (2002) 1331-1336.

[31] H. Cheng, N. Yang, Q. Lu, Z. Zhang, H. Zhang, Syntheses and Properties of Metal Nanomaterials with Novel Crystal Phases, Adv. Mater. 30(26) (2018) 1707189.

[32] G.N. Lewis, M. Randall, The Activity Coefficient of Strong Electrolytes, J. Am. Chem. Soc. 43(5) (1921) 1112-1154.

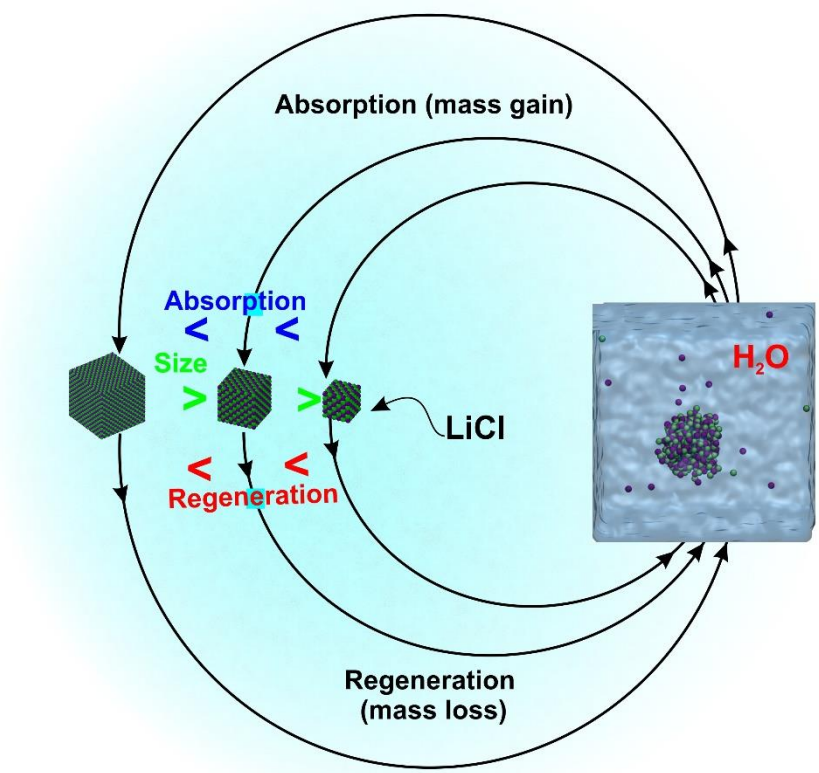

TOC: Nanocrystalline LiCl chemical reactivity